PROCEEDINGS OF SCIENCE

Medium-modified jet shape via transverse and longitudinal tomography

Yu-Xin Xiao,[a] **Yayun He,**[b,c] **Long-Gang Pang,**[a] **Xin-Nian Wang**[d] **and Hanzhong Zhang**[a,b,c,*]

[a] *Key Laboratory of Quark & Lepton Physics (MOE) and Institute of Particle Physics, Central China Normal University, Wuhan 430079, China*

[b] *Guangdong Provincial Key Laboratory of Nuclear Science, Institute of Quantum Matter, South China Normal University, Guangzhou 510006, China*

[c] *Guangdong-Hong Kong Joint Laboratory of Quantum Matter, Southern Nuclear Science Computing Center, South China Normal University, Guangzhou 510006, China*

[d] *Nuclear Science Division, Lawrence Berkeley National Laboratory, Berkeley, CA 94720, USA*

E-mail: zhanghz@mail.ccnu.edu.cn

Medium-modified jet shapes are investigated using a linear Boltzmann transport model for event-by-event simulations of γ-jet productions in heavy-ion collisions. The asymmetry ($A_N^{\vec{n}}$) localizes the initial transverse positions of the jets while the different selection of the jet transverse momentum (p_T^{jet}) exhibits the initial longitudinal positions. With the 2-dimensional jet tomography, our numerical results indicate that the in-cone transverse momentum is transported to the large angle away from the jet axis due to jet quenching in central Pb+Pb collisions at 5.02 TeV. Furthermore, the transverse momentum inside the jet cone behaves with an asymmetric distribution as the gradient of the jet transport coefficient ($\hat{q}$) increases.

HardProbes2023
26-31 March 2023
Aschaffenburg, Germany

*Speaker

PoS(HardProbes2023)168

1. Introduction

Jet quenching is an important probe to quark-gluon plasma (QGP) production in high-energy nucleus-nucleus collisions [1]. Compared with p+p collisions, large transverse momentum (p_T) hadrons or jets are greatly suppressed due to jet quenching in high-energy A+A collisions [2]. Theoretical studies show that jet quenching strength is proportional to jet transport coefficient ($\hat{q}$) [3] which is defined as the transverse momentum squared per unit length along the parton trajectory and is directly related to the medium gluon density. The nonuniform medium evolution can be described with the $\hat{q}$ gradient for the nonuniform jet quenching strength. A recent study [4] on γ-jets introduces an asymmetry observable $A_N^{\vec{n}}$ to localize the jets on the transverse sites of the jet moving direction, which gives a jet quenching gradient tomography to probe the medium. Our previous study [5] on γ-hadrons demonstrates a longitudinal tomography for the localized jet in the moving direction. The small p_T γ-hadrons are dominated by the fragmentation of partons created in the center region of the medium (volume emission) while the large p_T γ-hadrons are mainly contributed by the partons created in the outer corona region (surface emission). The 2-dimensional jet tomography helps to map the nonuniform properties of the QGP medium. So in this paper we use the 2D localization to check the medium modifications to jet shape in heavy ion collisions.

2. The theory model

The linear Boltzmann transport (LBT) model [6–10] was developed to study jet propagating in quark-gluon plasma in heavy-ion collisions and describe not only parton energy loss but also jet-induced medium excitation. Parton transport for both jet shower and thermal recoil partons in the hot medium obeys the linear Boltzmann equations. The elastic rate is calculated according to the leading order perturbative Chromodynamics, while the inelastic scattering rate is extracted from the high-twist approach [11, 12].

In our study we use PYTHIA 8 event generator [13] to generate the jet shower for γ-jet production events. The parton transports inside or outside the γ-triggered full jets are described by the LBT model. With the initial nuclear geometry given by a multiphase transport (AMPT) model [14], the CLVisc 3+1D viscous hydrodynamical model [15, 16] is used to give the information on fluid velocity and local temperature in the bulk medium to approach a more realistic evolution of QGP medium. We use the FastJet code package [17] with the anti-k_t jet algorithm to reconstruct full jets. In this work, we only use the partonic information for jet reconstruction to study jet shapes.

3. Numerical results

The jet shape gives the possibility density of transverse momentum distribution inside a jet cone, defined as [18],

$$\rho(r) = \frac{1}{\Delta r} \frac{\sum_i^N p_T^i (r - \Delta r/2, r + \Delta r/2)}{\sum_i^N p_{Ti}^{jet}}, \tag{1}$$

where the distance r between the track and the jet axis is defined as $r = \sqrt{(\eta - \eta_{jet})^2 + (\phi - \phi_{jet})^2}$ in the plane of pseudorapidity η and azimuthal angle ϕ, and Δr is the width of the radial

annulus with a inner radius between $r - \Delta r/2$ and $r + \Delta r/2$. $p_T^i = \sum_{assoc \in \Delta r} p_T^{assoc}$, and $p_T^{jet} = \sum_{assoc \in [0,R]} p_T^{assoc}$.

In the following calculations, we choose the trigger photon $p_T > 60$ GeV in 0-10% $Pb + Pb$ collisions at $\sqrt{s} = 5.02$ TeV at LHC. The cone size of the γ-triggered jets is set as $R = 0.3$, and the lower threshold of transverse momentum for the jets is $p_T^{jet} > 30$ GeV/c, in which the associated partons with $p_T^{assoc} > 1$ GeV are selected. The pseudorapidities for γ-jets are $|\eta_\gamma| < 1.44$ and $|\eta_{jet}| < 1.6$, and their azimuthal angles are constrained with $|\phi_\gamma - \phi_{jet}| > (7/8)\pi$.

3.1 Modified jet shape via 2D jet tomography

The asymmetry $A_N^{\vec{n}}$ is defined as[4],

$$A_N^{\vec{n}} = \frac{\int d^3r d^3k f_a\left(\vec{k},\vec{r}\right) \text{Sign}\left(\vec{k}\cdot\vec{n}\right)}{\int d^3r d^3k f_a\left(\vec{k},\vec{r}\right)}, \tag{2}$$

where the f_a is the phase-space distribution of partons and $\vec{n}$ is the normal direction of the reaction plane. It describes the collective transverse distribution of final particles. In the following calculations, we choose $\vec{n}$ along the y-axis, perpendicular to the reaction plane.

We calculate the jet shapes selected with the asymmetry A_N^y and initial transverse positions, respectively. Fig. 1 (left) are the ratios of jet shapes as a function of r between 0-10% $Pb + Pb$ (selected by different ranges of A_N^y from [-0.05, 0.05] to [0.65, 0.75]) and $p + p$ collisions at $\sqrt{s_{NN}} = 5.02$ TeV. Fig. 1 (right) are the ratios of jet shapes as a function of r between $Pb + Pb$ (selected by initial transverse positions y from [-0.5, 0.5] to [6.5, 7.5] fm) and $p + p$ collisions.

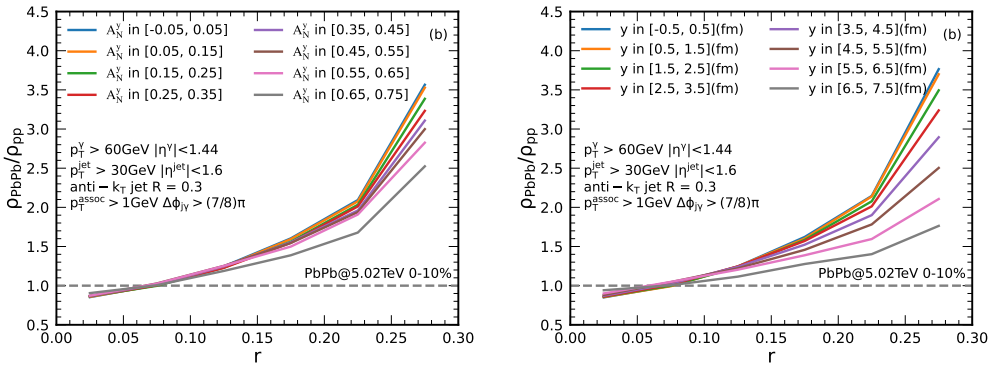

Figure 1: (Color online) The ratio of jet shape between 0-10% $Pb + Pb$ collision and $p + p$ collision as a function of r at $\sqrt{s} = 5.02$ TeV, selected by different A_N^y ranges (left) and initial jet production position y ranges (right), respectively.

Numerical results show that the final γ-jets selected by small A_N^y are more "fatter" than those by large A_N^y. Inside a "fatter" jet a significant fraction of the transverse momentum is transported to larger angles with respect to the jet axis due to stronger quenching for the central jets localized by small A_N^y. The similar results are also obtained in the selection case of given initial transverse positions.

Shown in Fig. 2 (left) is the jet shape as a function of r in 0-10% $Pb + Pb$ and $p + p$ collisions at $\sqrt{s_{NN}} = 5.02$ TeV in the upper panel, and the ratio of jet shapes between $Pb + Pb$ and $p + p$

collisions in the lower panel. The 3 different p_T^{jet} values are selected for event selections of γ-jets. We can conclude that contrasted to surface emissions, volume emissions encounter stronger medium effects and give the fatter jet shape.

Finally, simultaneously selected with both p_T^{jet} and A_N^y, the jet shapes of the γ-jets and the corresponding ratios between 0-10% $Pb+Pb$ and $p+p$ collisions at $\sqrt{s_{NN}} = 5.02$ TeV are shown in Fig. 2 (right). If both small A_N^y and p_T^{jet} are selected, the jet shape is fat due to volume emissions, while if both large A_N^y and p_T^{jet} are selected, the jet shape is thin due to surface emissions.

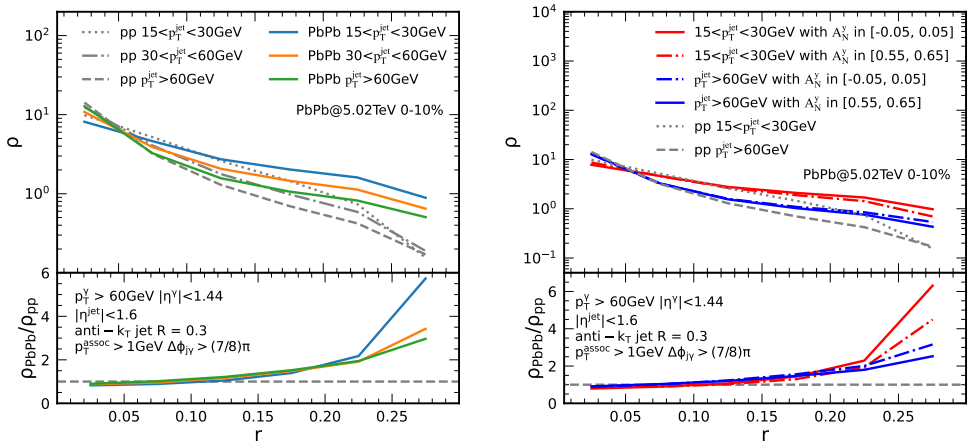

Figure 2: (Color online) Left figure shows jet shapes for $p+p$ and $Pb+Pb$ collisions which are selected by three p_T^{jet} ranges at $\sqrt{s} = 5.02$ TeV, the ratio of ρ_{PbPb} to ρ_{pp} are shown in lower panel. Right figure shows the jet shapes of $p+p$ collision selected by final p_T^{jet} and Jet shapes of $Pb+Pb$ collision select by both A_N^y and p_T^{jet} at $\sqrt{s} = 5.02$ TeV, the ratio of ρ_{PbPb} to ρ_{pp} are shown in lower panel.

3.2 Asymmetric jet shape

In above 2D tomography to medium modifications, somehow we focus on the p_T redistribution inside a jet, such as a fat or thin jet. Here we check the p_T asymmetry distribution inside a full jet.

We firstly divide the jet cone into the upper half cone and the lower half cone along "jet reaction plane". Here, the "jet reaction plane" is made up of jet-axis and z-axis. This plane is approximately parallel to the event reaction plane. The jet shapes of the upper half cone and the lower half cone are defined as,

$$\rho(r)_{upper/lower} = \frac{1}{\Delta r} \frac{\sum_i^N p_T^i (r - \Delta r/2, r + \Delta r/2) \Theta(+/-\vec{p}_T^{asso} \cdot \vec{n})}{\sum_i^N p_{Ti}^{jet}}, \tag{3}$$

where the positive sign in the Θ function is for ρ_{upper}, and the negative sign for ρ_{lower}.

The Fig. 3 (left) is for the ratio of ρ_{lower} over ρ_{upper}. The transverse momentum inside a jet cone is transported from small to large angles away from jet axis. Our numerical results show that such a transport is stronger in the lower half cone than in the upper half cone, especially the transport is stronger for a outer corolla jet than for a center jet. This implies that the jet shape is asymmetric.

To facilitate a better understanding of the p_T distribution and asymmetry within the jet cone, we introduce the following definition of ϕ_r,

$$\begin{cases} \phi_r = \arcsin(\Delta\eta/r), & (\Delta\phi \geqslant 0) \\ \phi_r = \pi - \arcsin(\Delta\eta/r), & (\Delta\phi < 0, \Delta\eta \geqslant 0) \\ \phi_r = -\pi - \arcsin(\Delta\eta/r), & (\Delta\phi < 0, \Delta\eta < 0). \end{cases} \tag{4}$$

The Fig. 3 (right) shows the p_T distribution as a function of ϕ_r. We choose three kinds of jets selected with A_N^y, respectively. They originate from three different locations inside QGP, for example, central and outer jets. For each jet, we check the angular p_T distribution of different regions inside each jet cone. The numerical results show that the center jet has a constant p_T distribution.

For the jet created in the outer layer of the medium, if close to the jet-axis, on the direction of $\phi_r = 0$, hard partons dominate the contribution to the p_T distribution peak. On the contrary, if away from the jet-axis, on the direction of $\phi_r = \pi$, it's soft partons that dominate the contribution to the p_T distribution peak. The jet quenching gradient results in the divorce of the hard and the soft centers inside the jet cone. In other words, the medium "kick" or $\hat{q}$ gradient pushes the hard transversely while the soft is reversely redistributed.

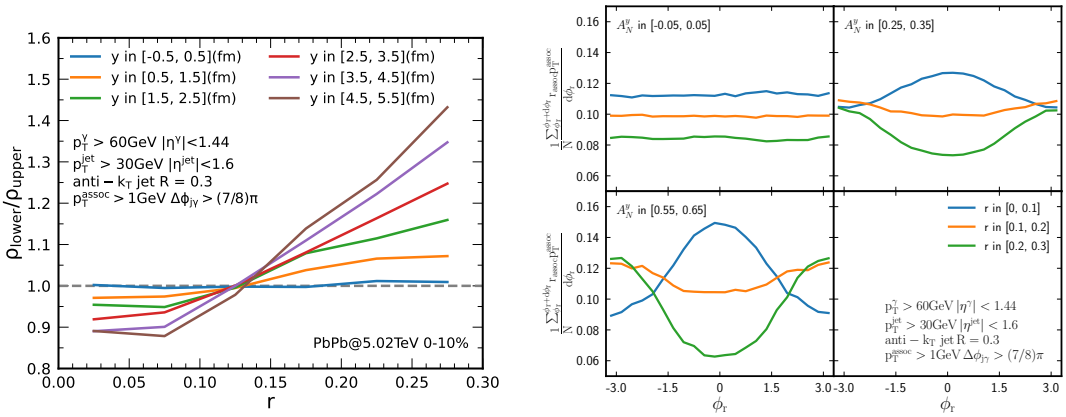

Figure 3: (Color online) Left figure shows the ratio of ρ_{lower} over ρ_{upper} as a function of r. Right figure shows the p_T distribution as a function of ϕ_r, which is weighted by r and selected with three different asymmetry regions, $A_N^y = [-0.05, 0.05]$, $[0.25, 0.35]$, and $[0.55, 0.65]$ in the three panels, respectively.

4. Conclusion

In this work, we employ the LBT model to study the jet shape of γ-jets for 0-10% $Pb + Pb$ collisions at $\sqrt{s_{NN}} = 5.02$ TeV. We study the medium-modified jet shape via transverse and longitudinal 2D tomography of γ-jets. Stronger jet quenching gives a fatter jet shape in which p_T transport is stronger towards the large angle with respect to the jet axis. The spatial gradient of $\hat{q}$ leads to an asymmetric jet shape of γ-jets. Inside a jet cone, medium "kick" or $\hat{q}$ gradient pushes the hard transversely, while the soft is reversely redistributed. The 2-dimensional localizations from the γ-jet tomography help to map the hot and dense medium properties with final observables.

Acknowledgments

This work is supported by National Natural Science Foundation of China under Grants Nos. 11935007, 11435004, Guangdong Major Project of Basic and Applied Basic Research No. 2020B0301030008, Science and Technology Program of Guangzhou No. 2019050001, and the Director, Office of Energy Research, Office of High Energy and Nuclear Physics, Division of Nuclear Physics, of the U.S. Department of Energy under Grant No. DE-AC02-05CH11231, the National Science Foundation (NSF) under Grant No. ACI-1550228 within the framework of the JETSCAPE Collaboration.

References

[1] M. Gyulassy and M. Plumer, *Phys. Lett. B* **243**, 432 (1990).

[2] A. Adare et al. (PHENIX Collaboration), *Phys. Rev. Lett.* **105**, 142301 (2010).

[3] R. Baier, Y. L. Dokshitzer, A. H. Mueller, S. Peigne, and D. Schiff, *Nucl. Phys. B* **483**, 291–320 (1997).

[4] Y. He, L.-G. Pang, and X.-N. Wang, *Phys. Rev. Lett.* **125**, 122301 (2020).

[5] H. Zhang, J. F. Owens, E. Wang, and X.-N. Wang, *Phys. Rev. Lett.* **103**, 032302 (2009).

[6] H. Li, F. Liu, G.-l. Ma, X.-N. Wang, and Y. Zhu, *Phys. Rev. Lett.* **106**, 012301 (2011).

[7] Y. He, T. Luo, X.-N. Wang, and Y. Zhu, *Phys. Rev. C* **91**, 054908 (2015), [Erratum: Phys. Rev. C **97**, 019902 (2018)].

[8] S. Cao, T. Luo, G.-Y. Qin, and X.-N. Wang, *Phys. Rev. C* **94**, 014909 (2016).

[9] X.-N. Wang and Y. Zhu, *Phys. Rev. Lett.* **111**, 062301 (2013).

[10] S. Cao and X.-N. Wang, *Rept. Prog. Phys.* **84**, 024301 (2021).

[11] X.-f. Guo and X.-N. Wang, *Phys. Rev. Lett.* **85**, 3591 (2000).

[12] B.-W. Zhang, E. Wang, and X.-N. Wang, *Phys. Rev. Lett.* **93**, 072301 (2004).

[13] T. Sjostrand, S. Mrenna, and P. Z. Skands, *JHEP* **05**, 026 (2006).

[14] Z.-W. Lin, C. M. Ko, B.-A. Li, B. Zhang, and S. Pal, *Phys. Rev. C* **72**, 064901 (2005).

[15] L. Pang, Q. Wang, and X.-N. Wang, *Phys. Rev. C* **86**, 024911 (2012).

[16] L.-G. Pang, H. Petersen, and X.-N. Wang, *Phys. Rev. C* **97**, 064918 (2018).

[17] M. Cacciari, G. P. Salam, and G. Soyez, *Eur. Phys. J. C* **72**, 1896 (2012).

[18] T. Luo, S. Cao, Y. He, and X.-N. Wang, *Phys. Lett. B* **782**, 707 (2018).